Characterization of Li Cations in Zeolite LiX by Solid-State NMR Spectroscopy and Neutron Diffraction

M. Feuerstein and R. F. Lobo*

Center for Catalytic Science and Technology, Department of Chemical Engineering, Colburn Laboratory, University of Delaware, Newark, Delaware 19716

Received February 26, 1998. Revised Manuscript Received April 30, 1998

Lithium cations in the dehydrated zeolites LiX-1.0 [$(SiAlO_4)_{96}Li_{96}$] and LiX-1.25 [$(Si_{106}Al_{86}O_{384})Li_{86}$] are characterized by a combination of neutron diffraction and magic-angle spinning (MAS) NMR spectroscopy. Both samples show in the ^{6}Li and the ^{7}Li MAS NMR spectra three lines assigned to Li cations in three different crystallographic sites (SI′, SII, and SIII′). The low-field component in ^{6}Li and ^{7}Li MAS NMR spectra recorded at a temperature of 295 K belongs to mobile Li cations, as proven by variable-temperature ^{7}Li MAS NMR spectra. Variable-temperature neutron diffraction experiments show a phase transition in the temperature range $T = 220-230$ K in case of LiX-1.0. Neutron diffraction data recorded at 296 K were refined in the cubic space group $Fd\bar{3}$ and data obtained at 20 K were refined in the orthorhombic space group *Fddd*. No phase transitions were observed in the refinement of the neutron diffraction data of zeolite LiX-1.25 ($Fd\bar{3}$) recorded at 10 K.

Introduction

For more than 20 years zeolites have been used industrially for gas separations, especially for the separation of nitrogen and oxygen from air using a process known as pressure swing adsorption (PSA).[1] Li-containing zeolites have been shown to be the most effective and selective adsorbents for N_2 adsorption.[2] Moreover, the nitrogen adsorption capacity of the LiX zeolites is strongly correlated with the amount of charge-balancing Li cations. Recently LiX and LiY zeolites have also been used for catalytic isomerization of olefins,[3] and LiX has been shown to have particularly larger ionic conductivities after exchange into the Li form.[4] This has served as a motivation to undertake an investigation of Li-exchanged zeolite X (zeolite faujasite).

To determine structure−property relationships of Li-exchanged zeolites it is necessary to determine the location of extraframework cations. In zeolites, classical X-ray diffraction techniques are usually used for this purpose, especially if single crystals are available. However, since most synthetic zeolites are formed as very fine polycrystalline products, powder diffraction techniques must be applied for structure analysis. Moreover, since a Li cation has only two electrons, it also has a small X-ray scattering cross-section. Due to this combination of factors, powder neutron diffraction methods are usually needed to determine the location of Li cations.

Previously, Forano and co-workers[5] studied a LiY (Si/Al = 2.4) and a LiX (Si/Al = 1.25) zeolite by neutron diffraction. The structures were refined in the space group *Fd*3*m*, i.e., Al and Si atoms where not distinguished crystallographically. Li cations were found in both samples at two different crystallographic sites. These are two sites in front of six-ring windows (SI′ inside the β-cages, SII inside the supercages), and a third position near the four-ring windows (inside the supercages at SIII) was found in LiX. These sites are depicted in Figure 1. Recently, Plevert et al.[6] reported a phase transition to *Fddd* (orthorhombic) in zeolite LiX-1.0 observed in the neutron diffraction data recorded at $T = 10$ K. Neutron diffraction data recorded at $T = 300$ K were refined in the cubic space group $Fd\bar{3}$. The authors found in both phases cations at the positions SI′, SII, SIII, and SIII′ (SIII′ cations are placed in the 12-ring windows close to position SIII). Due to the lower symmetry of *Fddd*, three SIII and three SIII′ sites were observed in the low-temperature phase of LiX-1.0.

Despite the relatively larger neutron scattering cross section of Li^+, the determination of the Li cation sites by neutron diffraction can also be complicated by several circumstances. For example, conductivity studies[4] have shown that the LiX zeolite is more conductive than other X zeolites containing cations other than Li. This suggests that some of the Li cations in zeolite LiX are mobile (vide infra). Second, the overall cross section (σ) of the ^{7}Li nucleus ($\sigma = 1.4$ b[7]) is much smaller in comparison to the other nuclei in the zeolite such as ^{16}O ($\sigma = 4.2$ b). Furthermore, the localization of Li cations by refinement of powder diffraction data can be further complicated for sites with low symmetry and a low occupation factor.

(1) Gaffney, T. R. Solid State Mater. Sci. **1996**, *1*, 75.
(2) Chao, C.; Sherman, J.; Mullhaupt, J. T.; Bolinger, C. M. Patent U.S. 5,413,625, 1995.
(3) Pitchumani, K.; Ramamurthy, V. *Tetrahedron* **1996**, *37*, 5297.
(4) Krogh Anderson, E.; Krogh Anderson, I. G.; Metcalf-Johansen, J.; Simonsen, K. E.; Skou, E. *Solid State Ionics* **1988**, *28−30*, 249.
(5) Forano, C.; Slade, R. C.; Krogh Anderson, E.; Krogh Anderson, I. G.; Prince, E. J. *Solid State Chem.* **1989**, *82*, 95.
(6) Plevert, J.; Di Renzo, R.; Fajula, F.; Chiari, G. *J. Phys. Chem. B*, **1997**, *101*, 10340.
(7) Lovesey, S. W. *Therory of Neutron Scattering from Condensed Matter;* Calderon Press: Oxford, 1986; Vol. 1, pp 17.

S0897-4756(98)00112-4 CCC: $15.00
Published on Web 06/09/1998

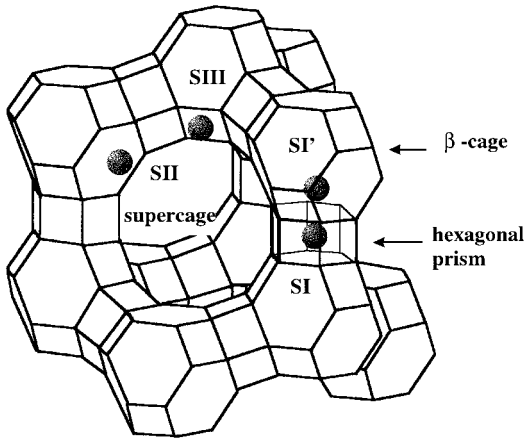

Figure 1. Cation positions in zeolite faujasite.

Because of the aforementioned potential problems, it is necessary to use another technique that complements the results from the neutron diffraction. Solid-state NMR spectroscopy is a very useful tool in this respect. For example, recently six components belonging to the six different crystallographic cation sites were observed by ^{23}Na MAS and ^{23}Na DOR NMR spectroscopy in zeolite NaX.[8] Both natural lithium isotopes (^{6}Li and ^{7}Li) are NMR-active nuclei. In comparison to other alkali metal cations, both ^{6}Li and ^{7}Li nuclei possess a small nuclear quadrupole moment (eQ), and, in particular, eQ for ^{6}Li is 50 times smaller than that of the naturally more abundant ^{7}Li nucleus.[9] The interaction of the electric quadrupole moment with the electric field gradient (EFG) is characterized by a quadrupole coupling constant (QCC) and asymmetry factor η, which describe the symmetry of the EFG. Since ^{6}Li is a spin $I = 1$ and ^{7}Li is a spin $I = {}^3/_2$ nucleus, lines in the ^{6}Li MAS NMR spectra are not broadened by second-order quadrupolar interaction. A disadvantage, however, is the very small chemical shift range observed for the Li nuclei. Xu and Stebbins[10] have recorded ^{6}Li MAS NMR spectra of several silicates and have observed isotropic shifts from $\delta_{iso} = -1.0$ ppm to $\delta_{iso} = 1.5$ ppm.

Previous NMR studies have been carried out on hydrated LiY or LiX zeolites[11] in which spin−lattice relaxation times were the main focus of the investigation. Lechert et al.[12] did model calculations of the quadrupole interaction of the ^{7}Li cations in zeolite X and reported broad band NMR studies of dehydrated LiX samples. The first ^{7}Li MAS NMR characterization of partially Li exchanged (maximum Li exchange of 70%) LiNaCaX zeolites (Si/Al = 1.2) was reported by Chezeau and co-workers.[13] The authors observed two or even three lines in the ^{7}Li MAS NMR spectra of dehydrated LiNaCaX zeolites, depending on the Li exchange. However, these lines were not assigned to different crystallographic cation sites in the zeolite structure. Feuerstein[14] studied a LiX-1.09 (Si/Al = 1 0.09) and a series of LiNaX zeolites by ^{7}Li and ^{23}Na MAS NMR spectroscopy, where he observed three lines in the ^{7}Li MAS NMR spectra assigned to Li cations in three crystallographic cation sites (SI′, SII, and SIII).

We report here the characterization of the zeolite LiX-1.0 and LiX-1.25 obtained by the combination of neutron diffraction and MAS NMR spectroscopy. ^{6}Li and ^{7}Li MAS NMR spectra of the deydrated LiX-1.0 and LiX-1.25 zeolites contain three lines belonging to Li cations in three different crystallographic sites (SI′, SII, and SIII). The results from the MAS NMR study are consistent with the refinement of the neutron diffraction data of these zeolites.

Experimental Section

Sample Preparation. NaKX (Si/Al = 1) zeolites were synthesized using a modification of the method reported by Kuehl.[15] First, a solution containing 15 g of sodium silicate and 15 g of deionized water was prepared. Second, 5.9 g of $NaAlO_2$, 7.1 g of KOH, and 9.9 g of NaOH were dissolved in 45 g of deinized water. Both solutions were mixed and stirred until the formation of a gel. Crystallization was carried out statically in Teflon containers starting at $T = 353$ K for 1 h and then at $T = 363$ K for 5 h. The as-synthesized form of the NaKX zeolite was throughly washed and dried in air at $T = 353$ K. Four cation exchanges were carried out with LiCl solutions at $T = 293$ K over 24 h. A 1 M LiCl solution was used for the first ion exchange, and 6 M LiCl solutions were used for the subsequent three exchanges.

Samples of NaX (Si/Al = 1.25) were obtained from commercial vendors (Aldrich, molecular sieve 13X). In this case the sodium form was exchanged six times with 1 M NH_4Cl solution at $T = 360-365$ K for 24 h to obtain the NH_4 form. The Li-exchanged zeolite LiX-1.25 was obtained by exchanging the NH_4 form three times with 1 M LiCl for 24 h and three times with 6 M LiCl at 365 K for 24 h. The absence of NH_4 was confirmed by IR using the KBr pellet technique. Full ion exchange was confirmed later by chemical analysis.

Partial ^{6}Li -exchanged samples of LiX-1.0 and LiX-1.25 were obtained by exchanging with a 1 M ^{6}LiCl solution for 24 h at $T = 293$ K. Dehydration was carried out by evacuating the sample below 10^{-1} Pa. At the beginning, the temperature was increased from $T = 300$ to 393 K with a heating rate 1 K/min and held at $T = 393$ K for 4 h. Later the temperature was increased to $T = 693$ K (heating rate 5 K/min) and kept there for 16 h. The completeness of dehydration was verified by ^{1}H MAS NMR spectra. Dehydrated samples for the MAS NMR characterization were prepared in 4 mm MAS NMR glass inserts (Wilmad Glass) and sealed while under vacuum. The sample studied by ^{7}Li satellite MAS NMR spectroscopy was packed under an argon atmosphere in a 4 mm MAS NMR rotor and not studied in sealed MAS NMR inserts. All the samples were checked by ^{27}Al MAS NMR spectra, and no extraframework aluminum was detected.

Analytical Section. MAS NMR spectra were carried out on a Bruker MSL 300 spectrometer operating at Larmor frequencies of 116.6 MHz for ^{7}Li and 44.2 MHz for ^{6}Li. The ^{7}Li satellite MAS NMR spectrum was recorded on a Bruker DSX-500 spectrometer ($\nu_0 = 194.4$ MHz). All the MAS NMR spectra were recorded with a 4 mm double-bearing MAS probe (Bruker) at spinning frequencies in the range of 5−10 kHz. Soft pulses with pulse lengths not longer than $\pi/8$ in case of ^{7}Li (spin $^3/_2$) were applied for the single-pulse experiments. For

(8) Feuerstein, M.; Hunger, M.; Engelhardt, G.; Amoureux, J. P. *Solid State NMR* **1996**, *7*, 95.
(9) Harris, R. K. *Nuclear Magnetic Resonance Spectroscopy*; Pitman: London, 1983; pp 250
(10) Xu, Z.; Stebbins, J. F. *Solid State NMR* **1995**, *5*, 103.
(11) Tokuhiro, T.; Iton, L. E.; Peterson, E. M. *J. Chem. Phys.* **1983**, *78*, 7473.
(12) Lechert, H.; Basler, W. D.; Henneke, H. W. *Ber. Bunsen-Ges. Phys. Chem.* **1975**, *79*, 563.
(13) Chezeau, J. M.; Saada, A.; Delmotte, L.; Guth, J. L. *Proceedings from the Ninth International Zeolite Conference*; van Ballmoos, R., Higgins, J. B., Tracy, M. M. J., Eds.; 1992.
(14) Feuerstein, M. NMR-spektroskopische Untersuchung zur Lokalisierung von Alkalimetallkationen (Li^+, Na^+, Cs^+) in dehydratisierten Zeolithen vom Faujasit-Typ., Dissertation, 1996.
(15) Kuehl, G. H.; *Zeolites* **1987**, *7*, 451.

Table 1. Information of the Neutron Diffraction Experiment of LiX-1.0 and LiX-1.25

Data Collection			
neutron facility	NIST	beamline	BT-1
monochromator crystal	Ge 311	wavelength (nm)	0.20784
step size (2θ, deg)	0.05		

	LiX-1.0		LiX-1.25	
expl conditions	$T = 296$ K	$T = 20$ K	$T = 295$ K	$T = 10$ K
space group	$Fd\bar{3}$	$Fddd$	$Fd\bar{3}$	$Fd\bar{3}$
a (Å)	24.6957	24.4819	24.6657	24.6763
b (Å)	24.6957	24.7648	24.6657	24.6763
c (Å)	24.6957	24.8978	24.6657	24.6763
no. of observation	2679	2679	2924	2843
no. of contrib reflctns	506	1499	558	540
R_{wp}	0.069	0.069	0.067	0.055
R_p	0.057	0.058	0.057	0.046
χ^2	1.43	1.68	1.60	1.96

the variable ^{7}Li MAS NMR experiments, a Bruker BVT-1000 unit was used.

Samples were characterized after synthesis and modifications by powder X-ray diffraction (XRD) using a Philips 3000 X'pert System with Cu Kα radiation. The neutron diffraction data were collected at the National Institute of Standards and Technology (NIST) research reactor on the BT-1 neutron diffractometer (wavelength of $\lambda = 0.2048$ nm). The neutron diffraction patterns were refined using the Rietveld program GSAS.[16] Peak shapes were simulated using the pseudo Voigt profile coefficients as parametrized by Thomson and coworkers[17] in combination with the asymmetry correction described by Finger et al.[18] The background was fitted to a shifted Chebyshev function. Data recorded for zeolite LiX-1.25 and the high-temperature phase of LiX-1.0 ($T = 296$ K) were refined in the cubic space group $Fd\bar{3}$, and the framework model (Si, Al, and O atoms) initially was used reported earlier by Olson.[19] Powder diffraction data of LiX-1.0 recorded at $T = 20$ K could not be indexed using the space group $Fd\bar{3}$ (see Results and Discussion). The data were refined using an orthorhombic structure model of lower symmetry ($Fd\bar{3}$). No changes in the symmetry were observed in case of the neutron diffraction data recorded at T = 10 K and T = 295 K for zeolite LiX-1.25 (space group $Fddd$). Structure models in all four refinements distinguished the crystallographic order of the Al and the Si atoms. The experimental conditions of these powder neutron diffraction refinements are summarized in Table 1.

In general, in the initial stage of the refinement only the zero-shift, scaling factor, background, lattice parameters, and profile parameters are optimized. In the second stage, the position of the framework atoms were optimized by using nonlinear soft constraints for the bond length (Si−O = 1.62 Å, Al−O = 1.73 Å). After this, positions of the Li cations were refined at SI′ and SII. At this point a difference Fourier synthesis was used to locate the remaining Li^+ cations. In the final stage of the refinement, all the parameters where fully refined and the geometric constraints were fully relaxed.

Results and Discussion

Neutron Diffraction. Figure 2 shows the results of the refinement of the neutron powder diffraction data of zeolite LiX-1.0 recorded at 296 K. The atomic positional parameters are summarized in Table 2. The agreement of the structural model and the experimental data is good ($R_{wp} = 0.068$, $R_p = 0.057$, $\chi^2 = 1.49$). The structural model contains three different Li sites: in front of the six-ring windows at SI′ and SII and near the four-ring windows inside the supercages at SIII. No Li cations were found at SIII′, as reported by Plevert et al.[6] Chemical analysis indicates the presence of a total of 96 Li cations per unit cell in LiX-1.0, and 88 of these cations could be located by the Rietveld refinement. Nearly complete occupation of sites SI′ and SII was observed (see Table 2). Site SIII is occupied by 23 cations and difference Fourier maps did not show any significant maxima that could be attributed to missing Li cations.

Interestingly, the temperature factor at SIII is much larger than the factors obtained for the SI′ and the SII

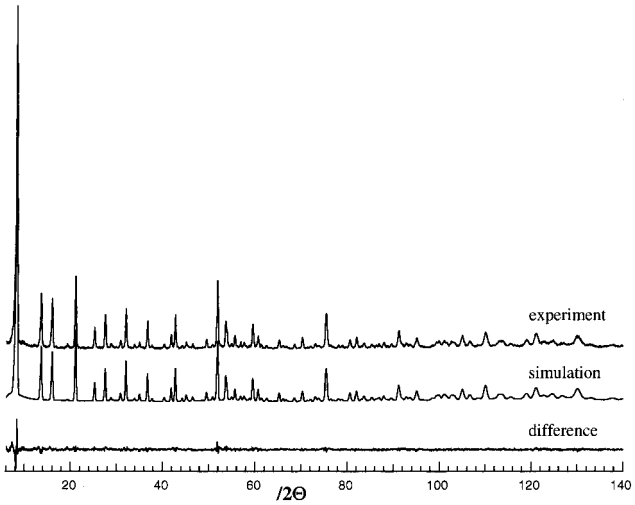

Figure 2. Neutron diffraction data of LiX-1.0 ($T = 296$ K).

Table 2. Structure Parameters of LiX-1.0 from Rietveld Refinement

atom	x	y	z	$U_{iso}/100$	PP
LiX-1.0 ($T = 296$ K), origin choice 2 at $Fd\bar{3}$					
Si	−0.0480(4)	0.1246(5)	0.0376(6)	1.9	96
Al	−0.0511(5)	0.0378(6)	0.1224(6)	1.9	96
O1	−0.1045(3)	0.0028(5)	0.0972(4)	2.7	96
O2	0.0001(4)	−0.0007(4)	0.1533(2)	2.7	96
O3	−0.0220(2)	0.0724(4)	0.0702(4)	2.7	96
O4	−0.0742(2)	0.0812(4)	0.1711(5)	2.7	96
Li1	0.0466(7)	0.0466(7)	0.0466(7)	5.8	31.3(1.3)
Li2	0.2232(5)	0.2232(5)	0.2232(5)	3.7	33.5(1.3)
Li3	0.387(5)	0.401(4)	0.122(3)	9.9	22.6(2.2)
LiX-1.0 ($T = 20$ K), origin choice 2 at $Fd\bar{3}$					
Si1	0.9503(5)	0.1235(6)	0.0386(5)	0.89	32
Si2	0.0378(5)	0.9534(6)	0.1238(5)	0.89	32
Si3	0.1218(5)	0.0392(5)	0.9553(5)	0.89	32
Al1	0.9474(6)	0.0353(5)	0.1252(6)	0.28	32
Al2	0.1255(5)	0.9507(5)	0.0368(5)	0.28	32
Al3	0.0359(5)	0.1228(5)	0.9513(5)	0.28	32
O1	0.8974(8)	0.9934(7)	0.0980(7)	0.96	32
O2	0.0982(7)	0.8966(6)	0.0013(8)	0.96	32
O3	0.9966(9)	0.0980(6)	0.8985(6)	0.96	32
O4	0.0004(6)	−0.0016(7)	0.1540(5)	0.96	32
O5	0.1547(4)	0.0015(6)	−0.0021(5)	0.96	32
O6	−0.0022(6)	0.1519(6)	0.0028(7)	0.96	32
O7	0.9748(5)	0.0729(6)	0.0726(6)	0.96	32
O8	0.0735(6)	0.9794(5)	0.0751(6)	0.96	32
O9	0.0691(6)	0.0688(6)	0.9819(5)	0.96	32
O10	0.9234(5)	0.0796(6)	0.1741(6)	0.96	32
O11	0.1724(7)	0.9248(6)	0.0825(6)	0.96	32
O12	0.0858(5)	0.1677(5)	0.9292(6)	0.96	32
Li1	0.0437(8)	0.0450(9)	0.0489(8)	0.38	28.9(1.1)
Li2	0.2270(8)	0.2234(7)	0.2245(9)	3.30	34.1(1.6)

(16) Larson, A. C.; van Dreele, R. B. *GSAS, Generalized Structure Analysis System*; Los Alamos National Laboratory: New Mexico, 1995.
(17) Thompson, P.; Cox, D. E.; Hastings, J. B. J. *Appl. Crystallogr.* **1987**, *20*, 79.
(18) Finger, L. W.; Cox, D. E.; Jephcoat, A. P. J. *Appl. Crystallogr.* **1996**, *27*, 892.
(19) Olson, D. H. *Zeolites* **1995**, *15*, 439.

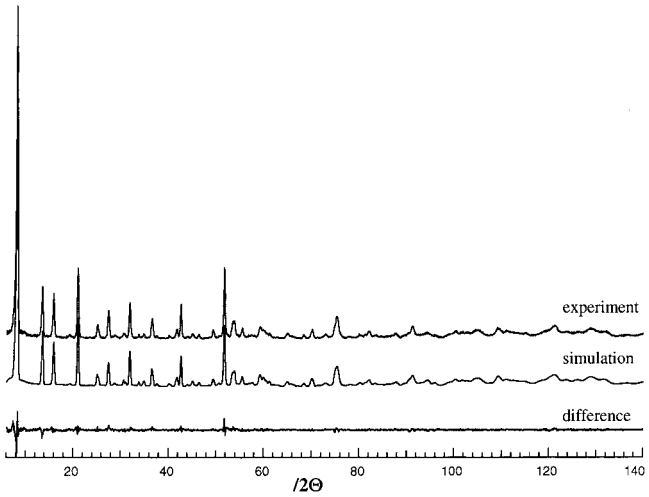

Figure 3. Neutron diffraction data of LiX-1.0 (T = 20 K).

cations. This observation suggests that the SIII cations are mobile or that static disorder causes an apparent increase in U_{iso}. We discuss this point in detail below when the refinement of the neutron diffraction data of LiX-1.25 is shown in combination with the ^{7}Li MAS NMR data. The large temperature factor for Li in SIII was also found by Plevert et al.,[6] but possible coupling between the population factors and thermal parameters was not discussed. Correlation between temperature and occupation factors may be the reason for the difficulty in locating the rest of the Li cations. ^{6}Li and ^{7}Li MAS NMR spectra of sample LiX-1.0 recorded at 293 K have shown that the line attributed to SIII correspond to 34 Li cations (see the following MAS NMR section). Hence, we have assumed that site population obtained by the ^{6}Li and ^{7}Li MAS NMR spectra represent the correct site population of SIII.

Neutron diffraction data were also recorded at lower temperature to reduce the motion of the SIII cations. Figure 3 shows the neutron diffraction data recorded at T = 20 K and the fitted model. The data could no longer be refined using a model in the cubic space group $Fd\bar{3}$ described above. Additional reflections indicate a phase transition to lower symmetry. The subgroups of $Fd\bar{3}$ were examined for a correct model to index the neutron diffraction data. Good agreement with experimental data resulted by fitting the experimental data in the orthorhombic space group $Fddd$, which lacks the 3-fold axis along hkl = 111. Therefore, the number of the Si, Al, and O atoms in the asymmetric unit increases by a factor of 3. Note also that the lowering of the symmetry increases peak overlap and reduces the amount of information that can be obtained from the powder pattern. At the same time, more structural parameters need to be refined. This phase transition has been reported by Plevert et al.[6]

Difference Fourier maps did not show any significant peak maxima belonging to the missing 32 Li cations near the four-ring windows inside the supercages. Peak minima and maxima in these difference Fourier maps have nearly the same absolute value, and it was decided to stop the refinement at this point. A model for the possible positions of the missing SIII cations will be given later in the text.

Several neutron diffraction data were recorded in the temperature range from T = 20 to 296 K to study the

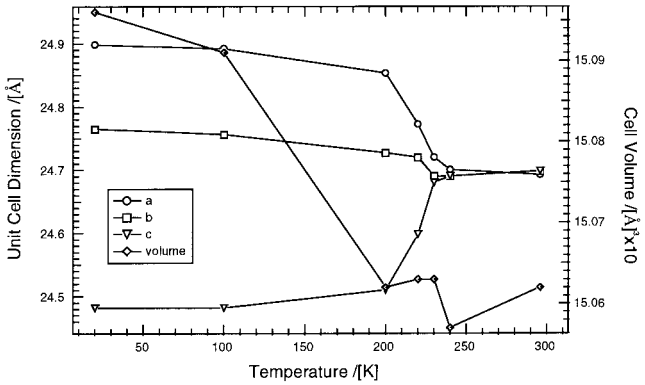

Figure 4. Temperature dependence of the unit cell dimension of LiX-1.0.

phase transition. Shorter collection times (by a factor of 4) were used in these data sets in comparison to the data collected at T = 20 K and 296 K. Due to the lower resolution, a complete Rietveld refinement was not attempted, and these powder patterns were fitted by the structural model obtained from the refinement of LiX-1.0 (T = 20 K). Only the zero-point, scaling factor, background parameters, profile parameters, and the lattice constants were refined. All other structural parameters were held fixed. Figure 4 shows the variation of the lattice parameters and the change in cell volume as a function of temperature obtained from this analysis. The phase transition is not very sharp and occurs over the temperature range from 220 to 230 K. Since lattice constants determined by neutron diffraction are of limited precision, we plan to study the phase transition by synchrotron diffraction. But it is worth noting, first, that there is almost no volume change during the phase transition (220−230 K) and, second, that the volume then slowly increases as the temperature is lowered. This is in contrast to the findings of Plevert,[6] where no volume change between 10 and 300 K was found. At this point we do not understand the source of this discrepancy.

Since as a result of the phase transition, it was not possible to obtain structural parameters for Li^+ in site SIII, a second sample of Li-exchanged X zeolite with higher Si/Al ratio was investigated. This sample does not show a phase transition at low temperatures. Neutron diffraction data of LiX-1.25 were recorded at 295 K and refined with the cubic structural model described above for LiX-1.0 (T = 296 K). One T site was 100% populated by Si atoms and for the other side a mixed population was assumed (85% Al and 15% Si).

Framework atomic and cationic positions were determined at SI′, SII, and SIII sites and were very similar to those of the previous sample. The zeolite composition is similar to the one of Forano and co-workers.[5] Unlike Forano et al.,[5] we considered the ordering of Si and Al atoms as reported earlier for X zeolites.[19] Forano and co-workers refined the structure in the space group $Fd3m$, with a higher symmetry than $Fd\bar{3}$ using a mixed population of Si and Al in the unique T site. Because of this difference, the location of Si/Al and framework oxygen atoms is significatively different. However, they found Li cations at positions comparable to our results. The main difference is the larger temperature factor of the SIII cations found in our

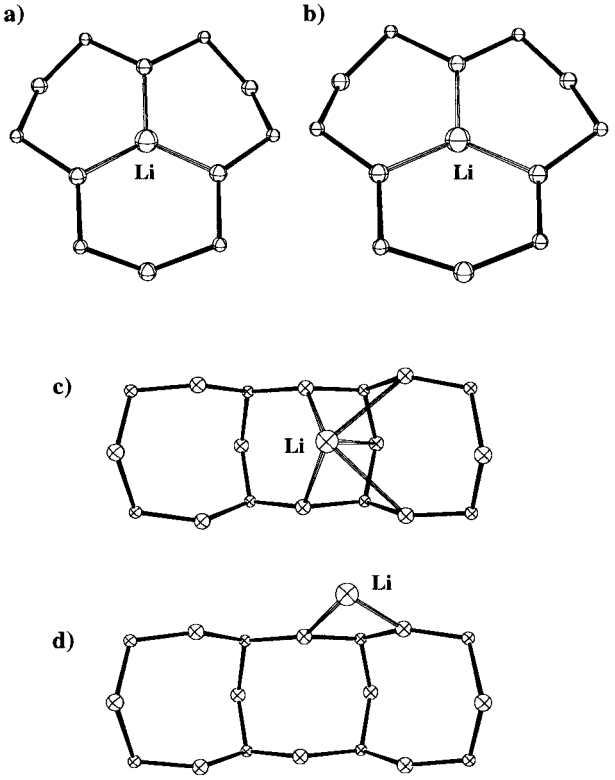

Figure 5. Position of the Li cations found at (a) SI′ (T = 296 K, LiX-1.0), (b) SII (T = 296 K, LiX-1.0), (c) SIII (T = 296 K, LiX-1.0), and (d) SIII′ (T = 10 K, LiX-1.25).

study. A similar result was found in the case of the SIII cations in zeolite LiX-1.0 (see above).

Neutron diffraction data of LiX-1.25 were additionally recorded at T = 10 K. It is interesting that no phase transition is observed for this zeolite, as in the case of LiX-1.0. The structure was also refined in the cubic space group $Fd\bar{3}$. The main difference between the data recorded at T = 295 K is in the position of the Li cations near the four-ring windows. These cations are no longer found in front of the four-ring windows (SIII) but are instead located inside the 12-ring windows (SIII′) at T = 10 K. This position is similar to the positions of the Na cations Olson[19] published for zeolite NaX-1.18 and Plevert et al.[6] found in LiX-1.0. The temperature factor of the Li cations at SIII′ did not show the large values observed for SIII at T = 295 K. However, SIII′ site population is lower than the one obtained from the simulation of the ^{6}Li and ^{7}Li MAS NMR spectra. This might be a hint for a second SIII′ position that cannot be found by analysis of difference Fourier maps.

The positions of the Li cations are depicted in Figure 5, as found by the refinement of the neutron diffraction data of zeolites LiX-1.0 and LiX-1.25. The location of the SI′ and SII cations did not vary significantly among the studied materials. Variation in temperature also did not affect these sites. Therefore, only these positions in zeolite LiX-1.0 at 296 K are shown.

Selected bond distances and angles are listed in Tables 3 and 5. We found in zeolite LiX-1.0 and LiX-1.25 average T−O (T = Si, Al) bond distances similar to distances Olson[19] reported for zeolite NaX-1.18. The average O−T−O (T = Si, Al) bond angles in both Li-exchanged X zeolites are 109.4°, as found for ideal tetrahedra.

Table 3. Selected Bond Distances and Angles of LiX-1.0

Bond Distances (Å) T = 296 K					
Si−O1	1.649	Al−O1	1.695	Li1−O3	1.902
Si−O2	1.651	Al−O2	1.755	Li2−O2	1.969
Si−O3	1.651	Al−O3	1.706	Li3−O4	1.893
Si−O4	1.628	Al−O4	1.710	Li3−O4	2.291
⟨Si−O⟩	1.645	⟨Al−O⟩	1.717		
Bond Angles (deg) T = 296 K					
Si−O1−Al	144.5	Si−O2−Al	127.0	Si−O3−Al	126.6
Si−O4−Al	136.7	⟨O−Si−O⟩	109.4	⟨O−Al−O⟩	109.5
Bond Distances (Å), T = 20 K					
Si1−O2	1.625	Si2−O3	1.625	Si3−O1	1.624
Si1−O6	1.627	Si2−O4	1.626	Si3−O5	1.625
Si1−O7	1.626	Si2−O8	1.626	Si3−O9	1.625
Si1−O10	1.626	Si2−O11	1.624	Si3−O12	1.625
Al1−O1	1.741	Al2−O2	1.740	Al3−O3	1.741
Al1−O4	1.742	Al2−O5	1.741	Al3−O6	1.742
Al1−O7	1.741	Al2−O8	1.742	Al3−O9	1.742
Al1−O10	1.740	Al2−O11	1.741	Al3−O12	1.740
Li1−O7	1.918	Li1−O8	1.897	Li1−O9	1.873
Li2−O4	1.969	Li2−O5	1.997	Li2−O6	1.959
⟨Si−O⟩	1.625	⟨Al−O⟩	1.741		
Bond Angles (deg) T = 20 K					
Si3−O1−Al1	144.9	Si1−O2−Al2	145.8	Si2−O3−Al3	145.1
Si2−O4−Al1	126.0	Si3−O5−Al2	125.0	Si1−O6−Al3	127.4
Si1−O7−Al1	131.4	Si2−O8−Al2	129.8	Si3−O9−Al3	122.6
Si1−O10−Al1	135.5	Si2−O11−Al2	132.3	Si3−O12−Al3	137.9
⟨O−Si−O⟩	109.4	⟨O−Al−O⟩	109.4		

Table 4. Structure Parameters of LiX-1.25 from Rietveld Refinement

atom	x	y	z	U_{iso}/100	PP
LiX-1.25 (T = 295 K), origin choice 2 at $\bar{3}$					
Si	−0.0476(4)	0.1233(5)	0.0372(6)	1.9	96
Al	−0.0508(5)	0.0374(6)	0.1237(6)	1.9	96
O1	−0.1017(3)	0.0023(5)	0.0994(4)	2.5	96
O2	−0.0001(4)	−0.0007(4)	0.1517(1)	2.5	96
O3	−0.0220(2)	0.0718(4)	0.0710(4)	2.5	96
O4	−0.0730(2)	0.0809(4)	0.1719(5)	2.5	96
Li1	0.0473(8)	0.0473(8)	0.0473(8)	2.2	25.6(1.2)
Li2	0.2230(9)	0.2230(9)	0.2230(9)	3.7	31.2(1.2)
Li3	0.387(2)	0.401(3)	0.122(2)	10.5	11.5(2.6)
LiX-1.25 (T = 10 K), origin choice 2 at $\bar{3}$					
Si	−0.0475(4)	0.1249(5)	0.0367(5)	1.32	96
Al/Si	−0.0513(5)	0.0377(5)	0.1226(5)	1.32	96
O1	−0.1020(3)	0.0004(6)	0.0977(3)	1.63	96
O2	0.0000(3)	0.0008(3)	0.1523(2)	1.63	96
O3	−0.0213(2)	0.0733(4)	0.0707(4)	1.63	96
O4	−0.0734(2)	0.0808(4)	0.1721(4)	1.63	96
Li1	0.0461(5)	0.0461(5)	0.0461(5)	0.58	23.5(1.6)
Li2	0.2233(4)	0.2233(4)	0.2233(4)	3.2	30.4(1.8)
Li3	0.333(2)	0.483(2)	0.127(3)	7.9	9.6(2.1)

It seems that the Li ions at SI′ and SII interact more strongly with the framework than Na ions, as reflected by a distortion of the six-ring windows. T−O−T angles belonging to O atoms in the six-ring windows coordinating Li cations are very narrow (⟨130°⟩). In zeolite NaX-1.18 the T−O-T angles were found in the range 134.8°−145.5°.[19] This observation underscores the compromise between flexibility and rigidity of the faujasite-type framework. Baur[20] has studied the framework mechanics of several zeolites and has distinguished between collapsing and noncollapsing tetrahedral frameworks. Noncollapsing structures such as zeolite faujasite (FAU)

(20) Baur, W. H. *Proceedings of the 2nd Polish-German Zeolite Colloquium*; Rozwadowski, M., Ed.; Nicholas Copernicus University Press: Torun, 1995.

Table 5. Selected Bond Distances and Angles of LiX-1.25

Bond Distances, Å (T = 295 K)					
Si−O1	1.629	Al−O1	1.699	Li1−O3	1.904
Si−O2	1.635	Al−O2	1.710	Li2−O2	2.000
Si−O3	1.649	Al−O3	1.708	Li3−O1	2.090
Si−O4	1.637	Al−O4	1.692	Li3−O3	2.446
⟨Si−O⟩	1.638	⟨Al−O⟩	1.702		
Bond Angles, deg (T = 295 K)					
Si−O1−Al	145.4	Si−O2−Al	128.8	Si−O3−Al	127.5
Si−O4−Al	138.3	⟨O−Si−O⟩	109.4	⟨O−Al−O⟩	109.4
Bond Distances, Å (T = 10 K)					
Si−O1	1.640	Al−O1	1.671	Li1−O3	1.894
Si−O2	1.644	Al−O2	1.725	Li2−O2	1.976
Si−O3	1.654	Al−O3	1.721	Li3−O1	1.807
Si−O4	1.625	Al−O4	1.709	Li3−O4	2.012
⟨Si−O⟩	1.641	⟨Al−O⟩	1.707		
Bond Angles, deg (T = 10 K)					
Si−O1−Al	147.4	Si−O2−Al	127.7	Si−O3−Al	126.9
Si−O4−Al	137.7	⟨O−Si−O⟩	109.5	⟨O−Al−O⟩	109.4

or zeolite A (LTA) have parts that can be stretched, while necessarily other parts are compressed, and vice versa. As a result, there is a limit to the flexibility of the framework, which is one of the underlying reasons for the interesting properties of these two zeolites. Similar to our results, Trouw and Richardson[21] found in Li-exchanged zeolite LTA a distortion of the six-ring windows that are occupied by Li^+ and observed a symmetry lowering in the structure of LiLTA from *Fm*3*c* to *I*4/*mcm*.

It is interesting to compare the positions of the SIII Li cations as found in zeolite LiX-1.0 (T = 296 K) and LiX-1.25 (T = 295 K) with the position SIII′ determined for LiX-1.25 at T = 10 K. Variable-temperature ^{7}Li MAS NMR spectra give evidence that the SIII cations are mobile at temperatures greater than T = 273 K (see the NMR section below). The SIII position determined by neutron diffraction at T = 295 K may actually be the average position of the lithium cation as it jumps between sites at opposite corners of the four-rings. Hence, we propose a model for the motion of the Li cations near the four-ring windows in which the cations are jumping between SIII′ sites.

This model is however not fully consistent with the refinement of the neutron diffraction data from LiX-1.25 recorded at T = 10 K. It requires a second SIII′ position at the opposite 12-ring window. It could be possible that more than one SIII′ site for the Li cations in zeolite LiX exists but that these sites cannot be found by refinement of the neutron diffraction data due to the small coherent cross section of the ^{7}Li nucleus. In this context it is interesting to compare structure refinements of zeolite NaX reported recently. Olson[19]found three different SIII′ sites in a single-crystal XRD structure refinement for the sodium cations in zeolite NaX-1.18. These sites were observed as two components in the ^{23}Na MAS NMR spectra of different NaX zeolites.[8] Two components having nearly identical environments show one joint component in the ^{23}Na MAS NMR spectra. Recently Vitale[22] and co-workers studied zeolite NaX (Si/Al = 1.2) under similar conditions by neutron diffraction and found only one SIII′ site for the Na cations. This refinement however is not consistent with the NMR studies.[8]

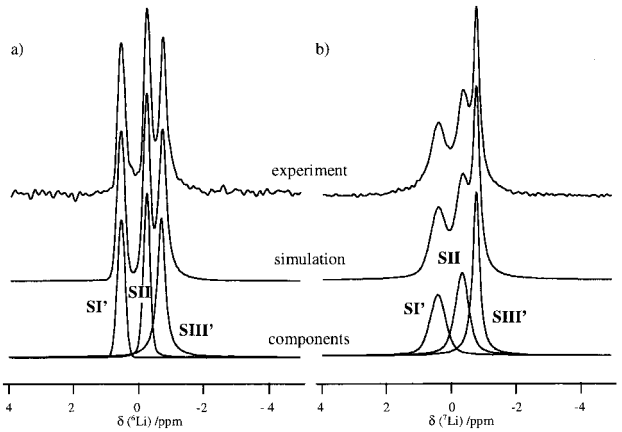

Figure 6. (a) ^{6}Li MAS NMR spectrum (ν_0 = 44.2 MHz) and (b) ^{7}Li MAS NMR spectrum (ν_0 = 116.6 MHz) of LiX-1.0.

MAS NMR Spectroscopy. ^{6}Li and ^{7}Li MAS NMR spectra of the dehydrated partially ^{6}Li-exchanged zeolite LiX-1.0 are depicted in Figure 6. The sample was prepared in MAS NMR glass inserts and sealed while under vacuum. Both spectra show three lines belonging to different crystallographic sites of Li cations in the zeolite, as reported earlier.[14] The parameters used for the simulation are summarized in Table 6.

Line assignments correspond with the results of the neutron diffraction data refinement described above. The low-field component, δ_{iso} = 0.4 ppm, is attributed to Li cations at SI′, the line at δ_{iso} = −0.3 ppm to SII cations, and the line at high field to SIII cations. The SI′ and SII components show Gaussian lines in the ^{6}Li MAS NMR spectrum, in contrast to the SIII line, which was deconvoluted with a Lorentzian line shape. This difference in the line shape is due to the mobility of SIII cations at T = 293 K. As mentioned above, the SIII cations show a much larger temperature factor in the Rietveld refinement than the SI′ and the SII cations. In addition, there is evidence for the mobility of the SIII cations from variable temperature ^{7}Li MAS NMR experiments (see below).

The SI′ and SII components are much broader in the ^{7}Li MAS NMR spectrum of zeolite LiX-1.0 than the SIII line because the cations are more strongly influenced by the quadrupolar interaction. The second-order quadruolar interaction can only be partly reduced by the use of the MAS NMR technique.[23] The SI′ and SII components were simulated by Lorentzian lines, but it is also possible to deconvolute these components by a quadrupole pattern broadened by Gaussian and Lorentzian functions. The line width and shape of the SIII line are nearly the same in the ^{6}Li and ^{7}Li MAS NMR spectrum. Therefore, the influence of the quadrupole interaction on the Li cations at SIII is generally very small.

A total of 96 Li cations per unit cell was determined by chemical analysis, and the site populations were obtained by the integrated line intensities in the ^{6}Li MAS NMR spectra. These site populations agree very

(21) Trouw, F. R.; Richardson, J. W., Jr. *Neutron News* **1997**, *8*, 22.

(22) Vitale, G.; Mellot, C. F.; Bull, L. M.; Cheetham, A. K. *J. Phys. Chem. B* **1997**, *101*, 4559.

(23) Rohr-Schmidt, K.; Spiess, H. W. *Multidimensional NMR and Polymers*; Academic: London, 1994.

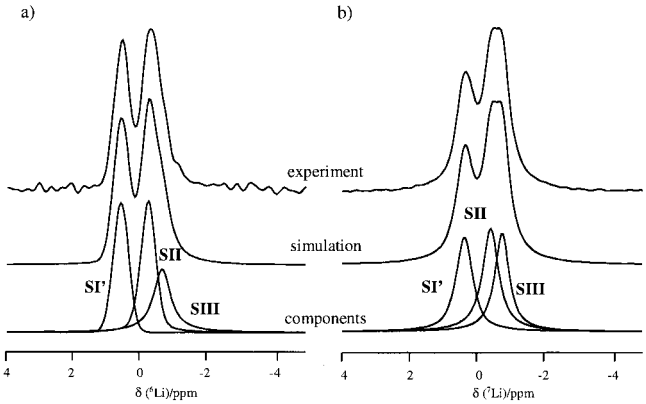

Figure 7. (a) ^{6}Li MAS NMR spectrum (ν_0 = 44.2 MHz) and (b) ^{7}Li MAS NMR spectrum (ν_0 = 116.6 MHz) of LiX-1.25.

Table 6. Parameters for the Simulation of ^{6}Li and ^{7}Li MAS NMR Spectra of Zeolites LiX-1.0 and LiX-1.25

		Li, uc	
position	δ_{iso}, ppm	NMR	ND
	LiX-1.0		
SI'	0.4	29	31.3(1.3)
SII	−0.3	33	33.5(1.3)
SIII	−0.7	34	22.6(2.2)
	LiX-1.25		
SI'	0.5	29	25.6(1.6)
SII	−0.3	32	30.4(1.8)
SIII	−0.7	24	11.5(2.6)

well within the accuracy limit of the method (estimated ±2 cations/unit cell) for SI′ and SII with the ones resulting from the Rietveld refinement (see Table 6); however, the site SIII population does not. The difference in the site population of SIII from NMR and neutron diffraction data is the result of the mobility of these cations. We think that under these circumstances it is likely that we are observing an artifact in the Rietveld refinement.

Line intensities in the MAS NMR spectra of noninteger quadrupolar nuclei like ^{7}Li ($I = {}^3/_2$), cannot usually be directly correlated with the crystallographic site populations. This is especially true if the spectra contain components with strong and weak quadrupole interaction. Intensities belonging to spinning sidebands of the central transition and to satellite transitions have to be considered.[24] However, the ratios of the line intensities in the ^{7}Li MAS NMR spectrum of zeolite LiX-1.0 correspond very well with the ones observed in the ^{6}Li MAS NMR spectrum.

The ^{6}Li and ^{7}Li MAS NMR spectra of zeolite LiX-1.25 are depicted in Figure 7. The sample was studied in sealed MAS NMR glass inserts as LiX-1.0 described above. The MAS NMR spectra were simulated with three components that belong to the cations at sites SI′, SII, and SIII. The line that belongs to the SIII cations (δ_{iso} = −0.7 ppm) shows a much smaller intensity in comparison to spectra of LiX-1.0. There are fewer Li cations at SIII because of the higher Si/Al ratio. These studies also showed good agreement between the Rietveld refinement and the MAS NMR results. As observed for LiX-1.0, the simulation of the ^{6}Li MAS NMR spectrum gives a larger occupation of site SIII than the Rietveld refinement.

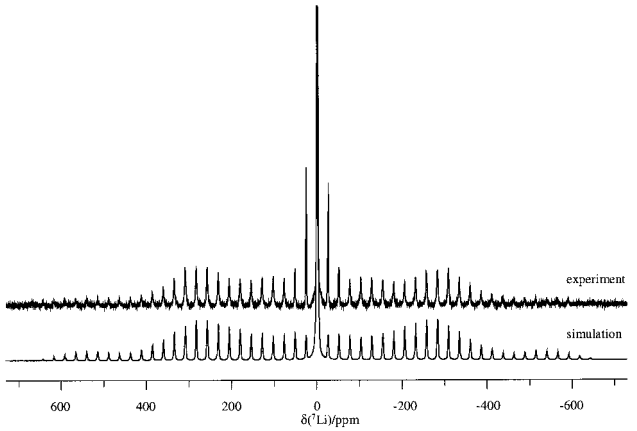

Figure 8. ^{7}Li MAS satellite spectrum (ν_0 = 194.4 MHz) of LiX-1.0 (ν_{rot} = 5 kHz).

Due to the small quadrupole interaction, no typical powder pattern was observed for the central lines in the ^{7}Li MAS NMR. Therefore, information about the quadrupole interaction is hidden. To obtain more details about quadrupole coupling constant (QCC) and the asymmetry parameter (η) we have applied ^{7}Li satellite MAS NMR spectroscopy[25] to the sample LiX-1.0.

Figure 8 shows the ^{7}Li satellite MAS NMR spectrum of the dehydrated zeolite LiX-1.0. Values of QCC = 0.25 MHz and η = 0.2 were obtained by the simulation of the rotational sidebands belonging to satellite transitions of the SII and SI′ component. These values agree very well with the data Lechert et al.[12] and ^{7}Li satellite MAS NMR spectra of a Li sodalite reported by Nielsen and co-workers.[26] The intensities of the inner sidebands were not fitted well by the simulations. This discrepancy may originate from spinning rates not fast enough to completely average the dipolar interactions, chemical shift anisotropy, or the sidebands caused by the second-order quadrupole interaction belonging to the central transition.

The information about the quadrupole interaction is very useful because the quadrupolar shift can be calculated and therefore the isotropic chemical shift can be obtained. These quadrupole parameters were used to calculate the quadrupolar shift δ_{qs} = −0.11 ppm in the ^{7}Li MAS NMR ($I = {}^3/_2$) spectra using the formula below:[27]

$$\delta_{qs} = -3 \times 10^5 \frac{QCC^2}{\nu_0^2} \frac{[I(I+1) - 3/4]}{[2I(2I-1)]^2}(1 + \eta^2/3)$$

This small quadrupolar shift is too small to be observed in the limit of the resolution of the MAS NMR spectrometer. Hence, the positions of the lines in the ^{7}Li MAS NMR spectra are taken as δ_{iso} and the quadrupolar shifts are neglected. For ^{6}Li (I = 1) the first-order quadrupolare shift is zero and only the second-order quadrupolare shifts have to be considered. Because of the much smaller nuclear quadrupole mo-

(24) Massiot, D.; Bessada, C.; Coutures, J. P.; Taulelle, F. *J. Magn. Reson.* **1990**, *90*, 231.

(25) Samoson, A. *Chem. Phys. Lett.* **1985**, *119*, 29. Skibsted, J.; Nielsen, N. C.; Bildsoe, H.; Jakobsen, H. J. *J. Magn. Reson.* **1991**, *5*, 88.

(26) Nielsen, N. C.; Bildsoe, H.; Jakobsen, H. J.; Norby, P. *Zeolites* **1991,** *11*, 622.

(27) Müller, D. *Ann. Phys. (Leipzig)* **1982**, *39*, 451.

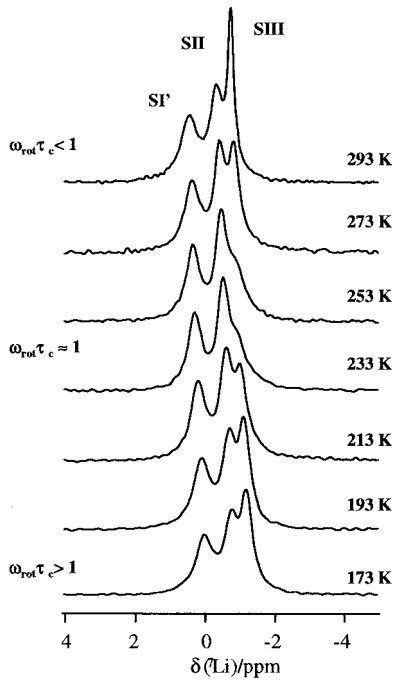

Figure 9. Variable-temperature ^{7}Li MAS NMR spectra of LiX-1.0.

ment in case of ^{6}Li, the quadrupolar shift is even smaller than that of ^{7}Li.

Variable-Temperature ^{7}Li MAS NMR Spectra. We have found an interesting effect of temperature on the ^{7}Li MAS NMR spectra. Figure 9 shows the variable-temperature ^{7}Li MAS NMR spectra of zeolite LiX-1.0. Temperature was measured by an uncalibrated element inside the MAS stator.[28] Therefore, at the low-temperature limit the sample temperature may be higher. The spectra recorded at $T = 273$ and 293 K show a narrow Lorentzian line at low field belonging to the Li cations at SIII. As the temperature is lowered ($T = 253 \rightarrow 233$ K), it is observed that this line broadens dramatically. At temperatures below $T = 213$ K the SIII line becomes narrow again and has a more Gaussian line shape than at room temperature.

Andrew and Jasinski studied the influence of microscopic motion on the line narrowing in MAS NMR spectra.[29] We interpret our results within their formulation of the theory. For the SIII lines at temperatures higher than $T = 273$ K, a narrow Lorentzian line is observed because the motion of the cations, characterized by the correlation time τ_c, is much shorter than the reciprocal of the rotation frequency ω_{rot}. In this limit, the motion of the SIII cations causes line narrowing. On the other hand, at temperatures below $T = 213$ K, τ_c is larger than $1/\omega_{rot}$ and the SIII lines are narrowed by MAS. The strong broadening in the middle temperature range ($T = 253-233$ K) is due to the fact that MAS NMR does not cause line narrowing when the motion of the cations is on the order of $1/\omega_{rot}$.

(28) Haw, J. *J. Anal. Chem.* **1988**, *60*, 559.
(29) Andrew, E. R.; Jasinski, A. *J. Phys. C* **1971**, *4*, 391.

Summary

In the present work, we have shown in detail the results of our study of Li cations in zeolites LiX-1.0 and LiX-1.25. A phase transition from $Fd\bar{3}$ (cubic) to *Fddd* (orthorhombic) has been observed in the temperature range $T = 220-230$ K by neutron diffraction for the sample with a lower silica content (LiX-1.0). ^{6}Li and ^{7}Li MAS NMR spectra of LiX-1.0 and LiX-1.25 were simulated by three components. Consistent with this result, Li cations were found in three crystallographic sites (SI′, SII, and SIII) by the refinement of neutron diffraction data. Interestingly, variable-temperature ^{7}Li MAS NMR spectra of LiX-1.0 have shown that site SIII, as found by the Rietveld refinement, represents an average of dynamically exchanging Li cations.

Adsorption experiments have shown that the X zeolites with high Li exchange rates show a higher nitrogen adsorption capacity.[1] It is well-known, on the other hand, that Li cations prefer sites in front of the six-ring windows[5] and that the SIII sites are only found to be occupied by lithium in samples with high Li content. In the context of our results, the adsorption capacity is correlated with the amount of Li cations at SIII.

Acknowledgment. The authors thank the Department of Chemistry and Biochemistry of the University of Delaware for access to the NMR spectrometer. We want to thank Professor Dybowski for his useful discussions and Dr. Hubert Koller for recording the ^{7}Li MAS satellite spectrum of LiX-1.0. We acknowledge the support of the National Institute of Standards and Technology, U.S. Department of Commerce, in providing the neutron research facilities used in this work. This work was supported by the DRP program of the state of Delaware and PRAXAIR.

CM980112D